Computational Design of Steerable Broadband MEMS Antennas

Morgan A. Roddy [1] and Magda O. El-Shenawee [2]

[1,2]Computational Electromagnetics Group
[1]Microelectronics-Photonics Program
[2]Department of Electrical Engineering
University of Arkansas, Fayetteville, AR, 72701, United States
morgan.a.roddy314@gmail.com, magda@uark.edu

Abstract: This paper describes the origins, improvements, and variations of a broadband microwave antenna that can be beam-steered by a micro-electromechanical system (MEMS). The steerable MEMS antennas of this work were comprised of a teardrop shaped planar inverted cone antenna (Td-PICA) on top of a monolithic silicon hinge structure and MEMS platform. The Td-PICA was successfully optimized and a bandwidth of 15.6 was achieved before integration with the MEMS platform. The Td-PICA was integrated with two variations of the MEMS platform giving the antennas one or two degrees of freedom of rotation. The maximum angle of rotation before mechanical failure of the proposed MEMS platform was calculated with closed form design equations and predicted to be 6.4° ± 0.8°. The optimized Td-PICAs were integrated and their operation was simulated with finite element analysis in Ansoft's High Frequency Selective Surfaces (HFSS) simulation software. The antenna on the one degree of freedom MEMS platform operated from 3.15 – 12.09 GHz with a center frequency of 7.62 GHz. The antenna on the degree of freedom MEMS platform operated from 26.53 – 55.95 GHz with a center frequency of 41.24 GHz.

Keywords: Antennas, Broadband, MEMS, Planar Inverted Cone Antenna, Steerable, Teardrop Antenna

1. Introduction

The presented steerable MEMS antenna was originally reported in [1]. The goal was to provide a broadband steerable antenna suitable for imaging applications. The devices consist of a planar antenna mounted on a silicon membrane. The membrane was etched to release the platform and create a gimbal hinge structure. A coplanar waveguide (CPW) transmission line traversed the hinge structure to feed the antenna. Prototypic devices were rotated using electrostatic actuation by placing a charged conductor under one edge of the antenna platform. The Coulomb force between the conductor and the charge displacement in the silicon platform provided the force to rotate the platform. The rotation of the platform in turn changes the orientation of the antenna in space and thus can be used to steer the antenna beam. A planar broadband antenna was selected to increase the potential usability of the devices. The steerable MEMS antenna design is interesting because of its compact size, beam steering capability, compatibility with standard MEMS fabrication technologies, and can be scaled to operate over a wide range of frequencies. In this work, the MEMS platform is modified to provide more rotational angles. The proposed MEMS platforms here are investigated independently and then integrated with the antenna. The current wok presents numerical design while no fabrication has been conducted yet.

2. Teardrop Planar Inverted Cone Antenna Optimization

The antenna selected for integration with the steerable MEMS platform is the teardrop planar inverted cone antenna (Td-PICA) [2 – 4]. The design is created by joining a half-dome monopole antenna with an inverted cone antenna and then smoothing out the edges. The resulting antenna is defined by a 32-point polyline that is normalized to have a total length and width of 1. This polyline is scaled in the X and Y directions for the purpose of optimization.

A. Basic Teardrop Planar Inverted Cone Antenna Form

A fully parameterized HFSS model of the Td-PICA has been created to optimize the antenna shape before integration with the steerable MEMS platform. The model consists of the Td-PICA on a silicon substrate with no ground and fed by a CPW. The design is optimized by changing the antenna width, the thickness of its substrate, and the dimensions of the CPW. The length of the teardrop is defined as *L*, as shown in Fig. 1, and is fixed at $L = 6.2\ mm$ for all cases studied. This variable can be used to scale the operational frequency of the antenna. This is achieved by scaling every X and Y coordinate of the polyline that defines the teardrop shape by the length *L*, and thus changing the physical and electrical size of the antenna. The width of the antenna is controlled by multiplying the dimensionless scaling factor *W*, by every X coordinate of the polyline defining the antenna. *W* is the ratio of the width to the length of the teardrop as shown in Fig. 1 and is tuned to improve broadband antenna performance. The CPW dimensions are also tuned to improve broadband performance. In Fig. 1, the width of the CPW center feed is defined as *F*. The width of the CPW ground is defined as *G*. The spacing between the CPW center feed and ground is defined as *S*. The thickness of the antenna substrate is defined as *h*. The relative permittivity of silicon used in the model is $\varepsilon_r = 11.9$. Fig. 1 shows how the Td-PICA and CPW are defined for optimization.

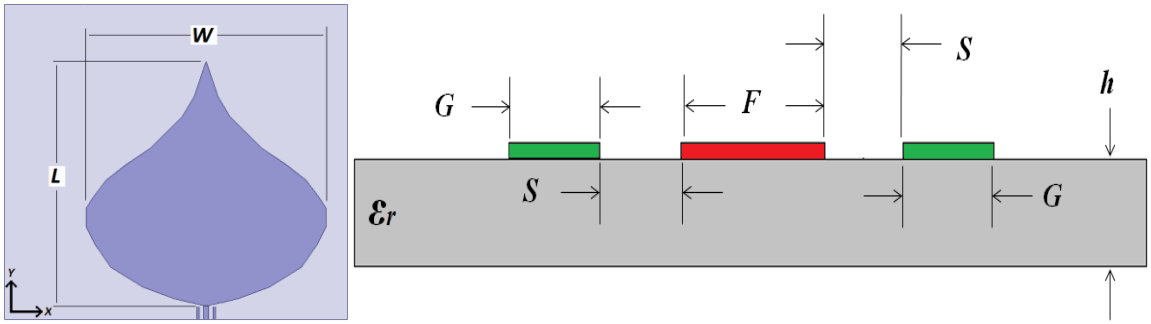

Fig. 1. Schematic of the Td-PICA and how it and the CPW are defined for optimization.

B. Optimization Results

The Td-PICA is optimized through variational analysis of the design variables *W*, *F*, *G*, *S*, and *h* in HFSS. The goal of the optimization is to maximize antenna bandwidth. This result is not necessarily a global maximum of performance, but is nonetheless remarkable. Designs are studied by creating a fully parameterized model of the antenna, substrate, and CPW feed. Parameters are sequentially varied and the resulting antenna performance observed and recorded for each variation. The variable *W* is first parametrically swept from *0.2 – 1.5* with a step size of *0.1* and the best bandwidth is observed when $W = 0.5$ and this value is retained. Next the variables *F*, *G*, and *S* are studied with a full factorial experiment where the values were $F = 7.5, 10, 12.5\ \mu m$, $S = 10, 15, 20, 26\ \mu m$, and $G = 7.5, 17.5\ \mu m$. The best bandwidth is observed when $F = 10\ \mu m$, $S = 20\ \mu m$, and $G = 7.5\ \mu m$ and these design values are retained. The variable *W* is again parametrically swept from *0.3 – 0.7* with a step size of *0.1* and a new best bandwidth is observed best case value of $W = 0.3$ was retained. Lastly, variable *h* is parametrically swept from *70 - 100* μm with a step size of *10* μm and the best bandwidth is observed when $h = 10\ \mu m$ and this value was retained. The optimized Td-PICA has a return loss below -10 dB

from 2.87 – 44.68 GHz which results in a bandwidth of 15.6. The antenna exhibits a typical monopole type radiation pattern with a gain of -12 dB at 10 GHz -7 dB at 40 GHz. The real and imaginary parts of the antenna input impedance and return loss of the optimized Td-PICA without the steerable MEMS platform are shown in Fig. 2.

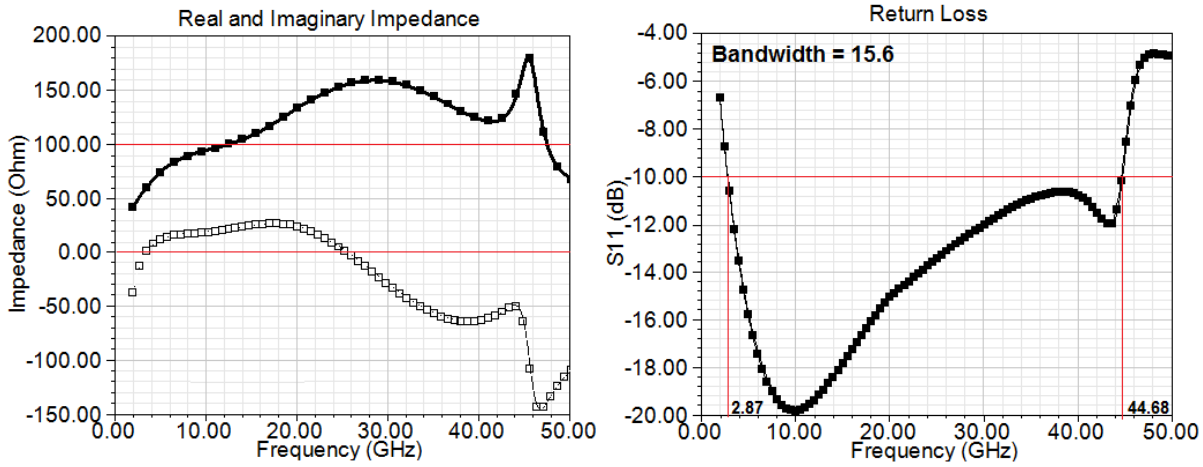

Fig. 2. Real and imaginary parts of the input impedance and return loss referenced to 100 Ω of the optimized Td-PICA.

3. The Steerable MEMS Antenna Platforms

The steerable MEMS antenna platform consists of a frame, torsion hinges, an intermediate frame, and the antenna platform. The device is designed to be created though the bulk micromachining of single crystal silicon. The platform is designed to support a planar antenna which was fed by a planar transmission line. Two variations are designed and studied that had one and two degrees of freedom of rotation respectively; the one and two degree of freedom (1D and 2D) platforms. The 1D platform has limited usefulness since it can only rotate in one dimension. The 2D platform can potentially have more applications but requires the CPW transmission line to have three 90° turns as it traverses the hinge structure. These discontinuities result in radiative losses. However, these losses are improved by replacing the 90° turns with pairs of compound 45° turns. Despite this improvement, the losses are still present so the 1D platform is useful to completely eliminate turns in the transmission line.

In both the 1D and 2D MEMS platforms, the hinges are designed to be three times thinner than the antenna platform and intermediate frame. This constraint was placed so it could be assumed that deformation is localized in the hinges when the devices rotate. This simplifies the mechanical analysis of the hinges and allowes for the use of closed for design equations. Both the 1D and 2D platforms are shown in Fig. 3. The different colors in the figure represent different thicknesses in the device. The frame was designed to be as thick as the silicon wafer used to create the device. The antenna platform and intermediate frame are designed to be three times thicker than the hinges.

The important performance metric of the hinge design is the maximum angle the antenna platform can rotate before mechanical failure. This rotation is a function of the hinge geometry and material properties. Since the deformation under rotation is assumed to be located in the hinges, they can be modeled as a rectangular torsion bar which has closed form design equations. Equation 1 is derived to predict hinge performance as a function of hinge geometry.

$$\theta_{fracture} = \frac{\tau_U \, l}{G\sqrt{\left(\frac{w}{2}\right)^2 + \left(\frac{t}{2}\right)^2}} \tag{1}$$

Where $\theta_{fracture}$ is the angle of rotation at which the device will fail, τ_U is the ultimate sheer stress in the

hinge, *l* is the hinge length, *w* is the hinge width, *t* is the hinge thickness, and *G* is the sheer modulus of silicon. This equation is used to study the effect of the hinge geometry on hinge performance. The value used in calculations for the ultimate sheers stress of silicon is $\tau_U = 1.15 \pm 0.15\ GPa$ [5]. The value used in calculations for the sheer modulus of silicon is $G = 79.4\ GPa$ [6]. The values for the hinge geometry parameters were $l = 1000\ \mu m$, $w = 76\ \mu m$, and $t = 20\ \mu m$. The resulting fracture angle calculated is $\theta_{fracture} = 6.4° \pm 0.8°$. This design variation of the hinges is used in the integrated antenna models for both the 1D and 2D variations of the antenna platform.

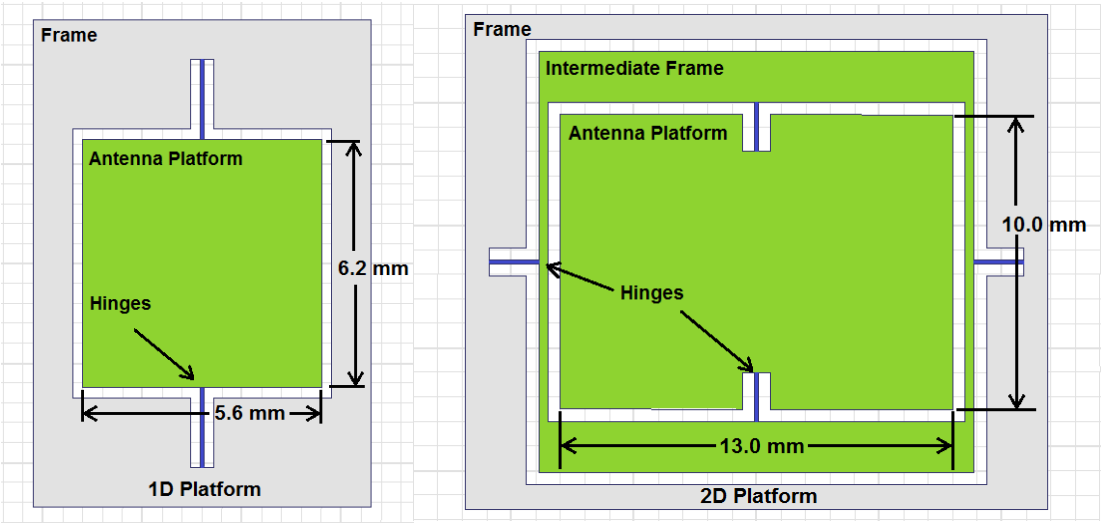

Fig. 3. The 1D and 2D MEMS antenna platforms.

4. Antenna/Steerable MEMS Platform Integration

Integrated models are created on the 1D and 2D versions on the steerable MEMS platform in HFSS. The optimized Td-PICA is used on both variations of the antenna platform. The simulation convergence limit is refined until two consecutive convergent passes had the same return loss curve. The most accurate simulation of the 1D version has 275,000 tetrahedrons resulting in a maximum delta S of 0.0004 at the solution frequency 26.5 GHz. The most accurate simulation of the 2D version has 675,000 tetrahedrons resulting in a maximum delta S of 0.0006 at the solution frequency 26.5 GHz. The simulations were run on the Razor supercomputer cluster at the University of Arkansas's High Performance Computing Center (AHPCC). The 1D Td-PICA operates from 3.15 – 12.09 GHz when referenced to 100 Ω, resulting in a bandwidth of 3.84 centered at 7.62 GHz. The 2D Td-PICA operates from 26.53 – 55.95 GHz 50 Ω resulting in a bandwidth of 2.11 centered at 41.24 GHz. The return losses of both antenna variations are shown in Fig. 4. The gain pattern of the 1D variation behaves like a monopole as in the Td-PICA optimization results with a gain of -16.3 dB at 3 GHz -4.6 dB at 40 GHz. The gain of the 2D variation does not have a regular monopole type radiation but rather had an irregular loped beam shape. The irregularity increased as frequency increased. The gain pattern of the 2D variation at 30 and 50 GHz is shown in Fig.5.

The Td-PICA has a remarkably large bandwidth before it is integrated with the MEMS platforms as shown in Fig. 2. The radiation pattern before integration is a stable monopole shape over a wide range of frequencies. As anticipated, the bandwidth is degraded upon integration with the MEMS platform. The bandwidth is reduced by almost 75% in the 1D variation and by 86% in the 2D variation. The bandwidth is reduced because the input impedance of both integrated antennas are not as stable over a wide range of frequencies as estimated in the optimized Td-PICA as shown in Fig 2. The gain shape does not change in the 1D variation after integration but is degraded to have numerous lobes in the 2D variation as shown in

Fig. 5. The degradation of the gain pattern from the optimized antenna to the 2D integrated variation can be attributed to the wave coupling with MEMS platform. The addition of the additional silicon structure of the MEMS platform and transmission line discontinuities is the source of radiative loss which changes the gain pattern. In conclusion, the addition of the MEMS platform gives the Td-PICA the characteristic of steerability at the cost of bandwidth and gain pattern.

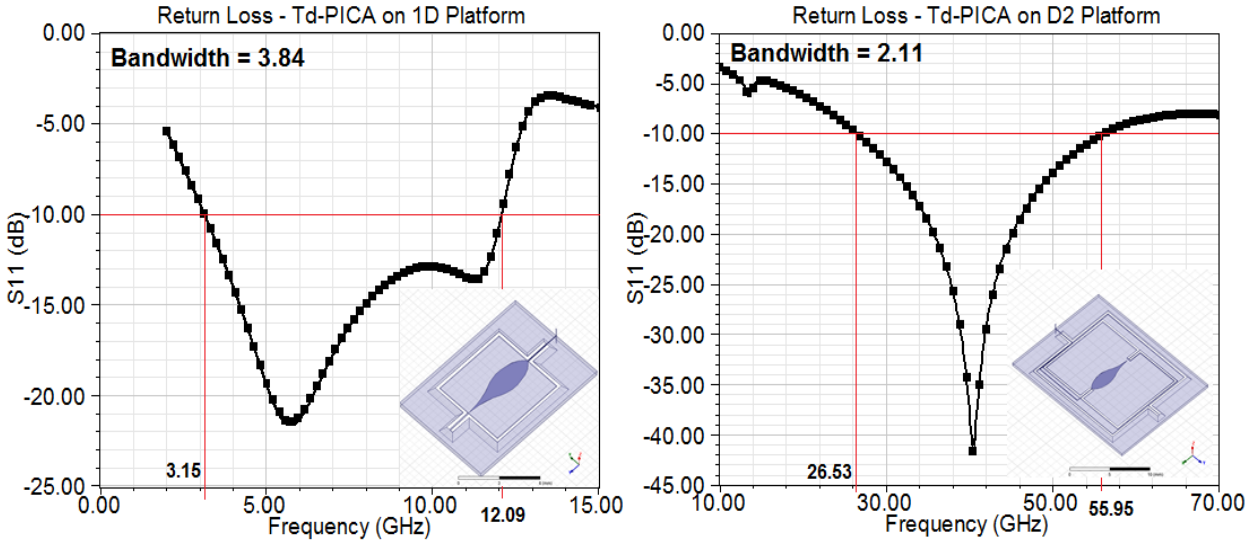

Fig. 4. Return loss of the Td-PICA on the 1D and 2D antenna platforms.

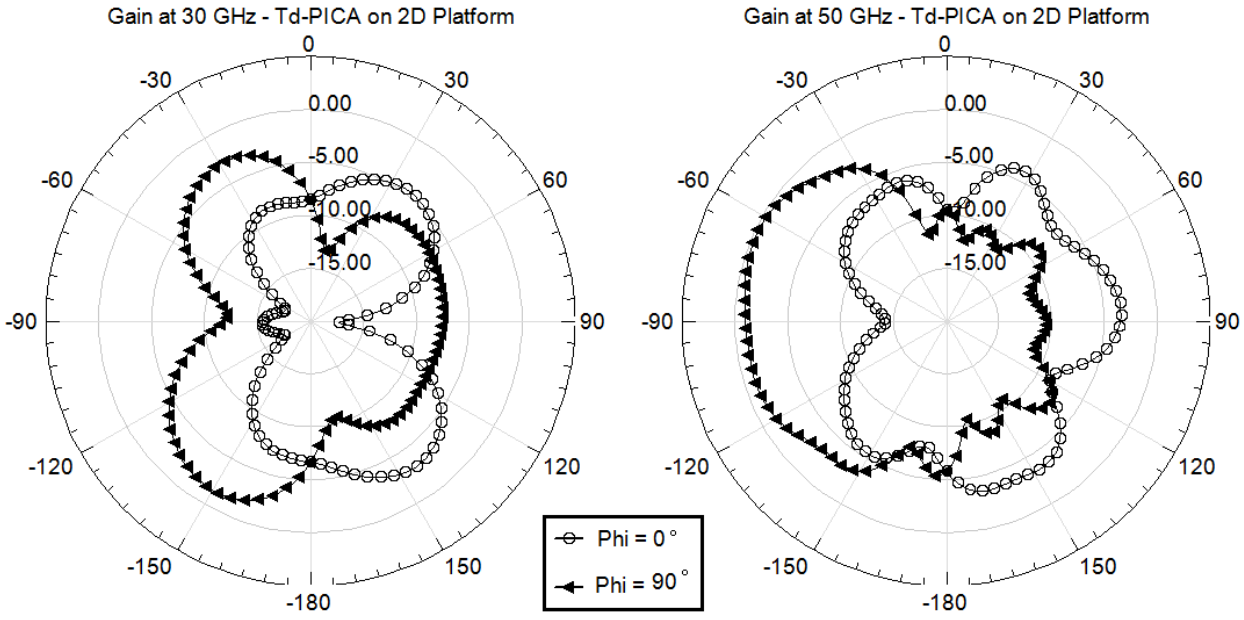

Fig. 5. Gain pattern of the Td-PICA on the 2D antenna platform at 30 and 50 GHz.

5. Conclusion

Two variations of the broadband steerable MEMS antenna were designed and studied primarily in HFSS. A new antenna design, the planar inverted cone antenna, was successfully optimized and a bandwidth of 15.6 was achieved before integration with the antenna platform. Two versions of the

antenna platform were developed as a tradeoff between antenna performance and degrees of freedom. The antenna with two degrees of freedom of rotation had a lower bandwidth than that with only one degree of freedom. The 1D antenna/platform variation had low radiative losses compared the 2D variation due to the absence of 90° turns or compound 45° turns. Additionally, standing waves in the 2D variation's transmission line caused the antenna to operate at much higher frequencies than the 1D.

Acknowledgement

The authors would like to acknowledge the Army Research Laboratory for their support. This work was completed under Cooperative Agreement Number W911NF-10-2-0093. The views and conclusions contained in this document are those of the authors and should not be interpreted as representing the official policies, either expressed or implied, of the Army Research Laboratory or the U.S. Government. The U.S. Government is authorized to reproduce and distribute reprints for Government purposes notwithstanding any copyright notation herein.

References

[1] D.A. Hutchings, *Design, Testing, and Fabrication of a Broadband MEMS Antenna*, University of Arkansas, 2010.

[2] S.-Y. Suh, *A Comprehensive Investigation of New Planar Wideband Antennas*, Virginia Polytechnic Institute and State University, 2002.

[3] S.-Y Suh, W. Stutzman, W. Davis, A. Waltho, J. Schiffer, "A novel broadband antenna, the low profile dipole planar inverted cone antenna (LPdiPICA)", *IEEE Antennas and Propagation Society International Symposium*, 2004, Volume: 1.

[4] E. Lule, T. Babij, K. Siwiak, "Elliptical slot tuned planar teardrop ultra wideband dipole antenna", *IEEE Antennas and Propagation Society International Symposium*, 2005, Volume: 2A.

[5] M. Ogawa, Y. Isono, "Novel Sheer Strength Evaluation of MEMS Materials Using Asymmetrical Four-Point Bending Technique", *20th IEEE International Conference on MEMS*, Kobe, Japan, January 2007.

[6] J. Kim, D. Cho, and R. Muller, "Why is (111) silicon a better mechanical material for MEMS", *Proc. Transducer*, Munich, Germany, June 2001, pp. 662–665.